



Title	An Experimental Study on the Main Flame Stability of a Premixed Concentric Jet Flame
Author(s)	Ito, Kenichi; Tatsuta, Setsuo; Takahashi, Fuyuhiko
Citation	北海道大學工學部研究報告, 105, 19-28
Issue Date	1981-07-31
Doc URL	http://hdl.handle.net/2115/41694
Type	bulletin (article)
File Information	105_19-28.pdf



[Instructions for use](#)

An Experimental Study on the Main Flame Stability of a Premixed Concentric Jet Flame

Kenichi ITO*, Setsuo TATSUTA* and Fuyuhiko TAKAHASHI*

(Received March 31, 1981)

Abstract

The blow-off mechanism of the main flame in a premixed concentric jet flame with a recirculation zone was studied experimentally. The detailed thermal structure of the recirculation zone and the chemical reaction processes at flame necking region between the recirculation zone and the main flame were examined. Propane-air mixture was ejected from a burner nozzle which had an inner diameter of 12 mm and a rim thickness of 7.5 mm, and a parallel air flow surrounded the burner nozzle coaxially.

In the case of a stable flame, it was found that the maximum temperature in the recirculation zone was located in the downstream region, and that the burning fraction at the flame necking region decreased near the conditions where the main flame blew off. The results of fluctuating temperature measurements at the flame necking region showed that RMS values had two peaks at both mixture side and parallel air side in the stable flame, while there was no peak at the mixture side with the near blow-off flame.

1. Introduction

In our previous paper, it was found that the premixed concentric jet flame was held by the recirculation zone formed behind the thick rim, and the flame stability depended on the heat transfer caused by mass exchange from the recirculation zone to the outer flows.^{1),2)} In such a flame, combustion occurs only inside the recirculation zone, namely, the main flame blows off, when a fresh mixture is rich and flow velocities are high. This type of flame is called crown flame, and was observed by Samia,³⁾ Mizutani et al⁴⁾, and Minx et al⁵⁾ in a diffusion concentric jet flame. However, no studies have been carried out on the blow-off mechanism of the main flame both in the case of premixed flame and diffusion flame.

The blow-off of normal flame which has both a recirculation zone and a main flame depends on the burning fraction in the recirculation zone.⁶⁾ The mean real mixing

* Department of Mechanical Engineering

ratio in the zone is a most dominant factor. On the other hand, it is considered that the blow-off of the main flame depends on the breaking-off of flame propagation at the flame necking region between the recirculation zone and the main flame. In this region, the flame front is formed in the boundary between the fresh mixture flow and the parallel air flow. Then, in order to clarify the blow-off mechanism, it is necessary to evaluate the performance of the recirculation zone as a heat source to the outer flows, and to examine the reaction processes at the flame necking region.

In this paper, the blow-off limits of the main flame were measured, and the relations between the main flame stability and the thermal structure of the recirculation zone were examined. Measurements of chemical species, mean and fluctuating gas-temperature were made at the flame necking region. The temperature fluctuation was measured by using a fine bare wire thermocouple which compensated the effect of thermal inertia. Root mean square (RMS) and probability density function (PDF) of temperature fluctuation which would be related to the blow-off were obtained.

2. Experimental Apparatus and Procedure

2.1 Apparatus

A schematic diagram of the experimental apparatus is shown in Fig. 1. Fuel used here is LPG (C_3H_8 ; 97.8 vol%, C_4H_{10} ; 2.2 vol%), and is premixed with the primary air in the mixing chamber. The fresh mixture is carried to the burner nozzle, which has an inner diameter of 12 mm and a rim thickness of 7.5 mm. Parallel air flow surrounds the burner nozzle coaxially. The velocities of the mixture U_{mix} and of the parallel air U_2 can be continuously controlled up to 120 m/s and 100 m/s, respectively. The combustion chamber consists of the working section for measurement and the duct section as shown in Fig. 1.

2.2 Measurement of mean gas-temperature and chemical species

The mean temperature is measured by an $100\ \mu\text{m}$ Pt-Pt/Rh 13 % thermocouple. Catalytic action is eliminated by coating the thermocouple with $(SiO_2)_x$. The radiation and conduction errors are not corrected. Species concentrations are measured by means of gas-chromatography. Gas for analysis is sampled with a quartz glass tube with an inner diameter of 0.3 mm.

2.3 Measurement of fluctuating gas-temperature

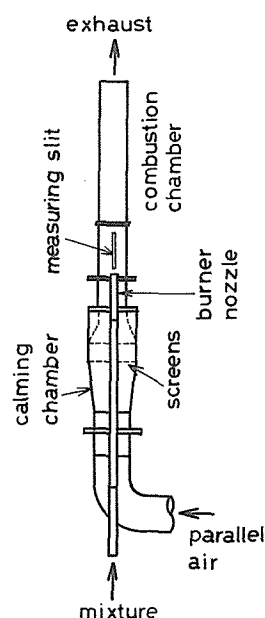


Fig. 1 Schematic diagram of experimental apparatus

The configuration of the probe used to measure the fluctuating temperature is shown in Fig. 2. A fine Pt-Pt/Rh 13 % thermocouple with a diameter of $50 \mu\text{m}$ was connected to the two prongs of a fork constructed from $300 \mu\text{m}$ wire of the same material. The thermocouple is not coated because of thermal inertia considerations.

The principle for the fluctuating temperature measurement was described first by Shepard et al.⁷⁾ It is to compensate the effects of the thermal inertia of the thermocouple by using an electric circuit, assuming that the frequency response characteristic of the thermocouple has a first order-lag in temperature signals. The temperature of the thermocouple $T_{th}(t)$ in the gas of temperature $T_g(t)$ is shown as follows.

$$T_g = T_{th} + \tau_{th} \left(\frac{dT_{th}}{dt} \right)$$

where τ_{th} is the thermocouple time constant. The value of τ_{th} depends on gas temperature and gas velocity. Therefore, by using the electric compensating circuit which performs upon the thermocouple emf $E_{th}(t)$, the operation $(E_{th} + \tau_c \frac{dE_{th}}{dt})$, and matching circuit time constant τ_c to τ_{th} , emf corresponding to the gas-temperature can be obtained.

A schematic diagram of the compensating circuit is shown in Fig. 3. It consists of a pre-amplifier, LPF, inverting amplifier, differentiation circuit and summing amplifier. The frequency response characteristics of the compensating circuit are shown in Fig. 4. The circuit time constant τ_c is adjustable in the range of 0~47 msec. and the bandwidth of circuit ranges from DC~2 KHz.

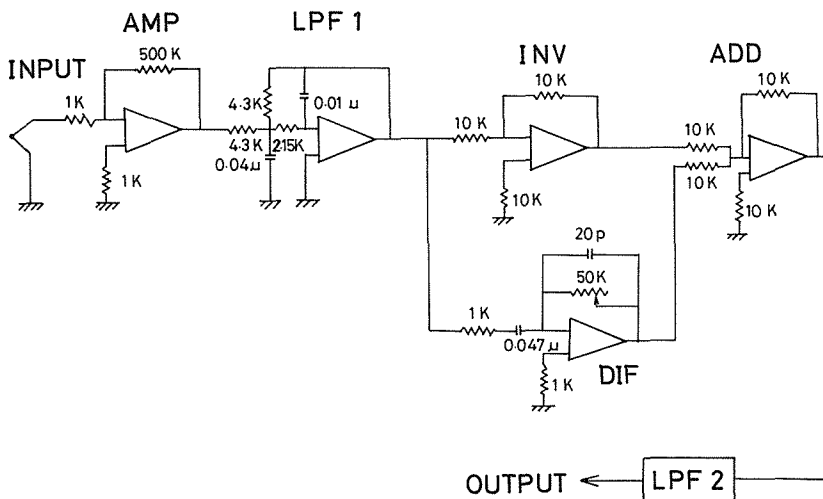


Fig. 3 Schematic of compensating circuit

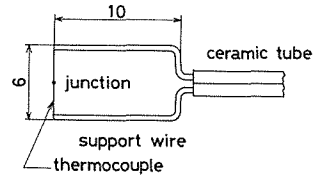


Fig. 2 Configuration of probe for fluctuating temperature measurement

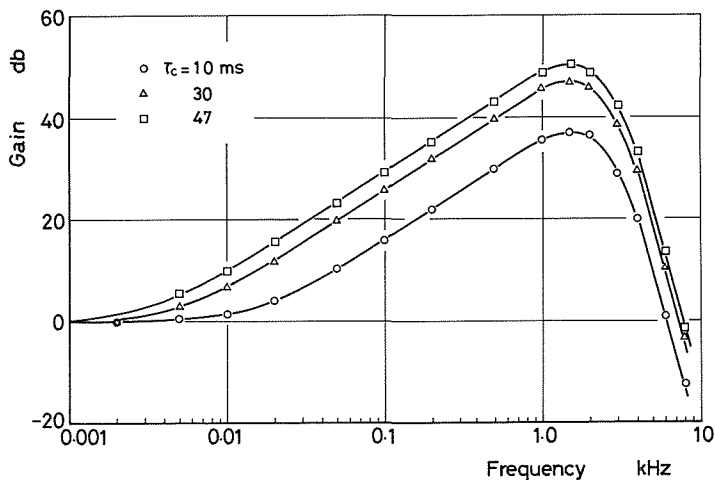


Fig. 4 Frequency response of compensating circuit

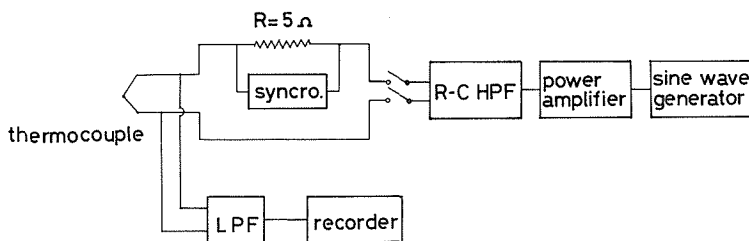


Fig. 5 System for thermocouple time constant measurement

The system for thermocouple time constant measurements is shown in Fig. 5. Alternating current with a frequency of 50 KHz is fed to the thermocouple to maintain its temperature at about 100 K above the gas-temperature. The thermocouple time constant τ_{th} is determined by the relations between the current amplitude I and the temperature rise ΔT_{th} . In the flame, gas-temperature and velocity fluctuate instantaneously, so that τ_{th} also fluctuates. Therefore, it is difficult to match τ_c to τ_{th} . In this study, the mean value of τ_{th} was used as τ_c .

3. Results and Discussion

3. 1 Main flame stability limits

Main flame stability limits, when parallel air velocity U_2 is kept constant at 35 m/s, is shown in Fig. 6. In this figure, U_{mix} is the mixture velocity and ϕ_{AF} ((Air/Fuel)/(Air/Fuel)_{st}) is the air-fuel equivalence ratio of the fresh mixture. The flame exists between the lower and the upper blow-off lines. The shapes of the flame are mainly distinguished into two types, an inner flame and an outer flame, by the position of flame fronts in the recirculation zone³⁾. The flame fronts in the flame base are located near the inner edge of the rim for the inner flame, and the outer edge for the outer flame. When ϕ_{AF} is small and U_{mix} is high, a crown flame is formed. In the case of

crown flame, most of the mixture fed to the burner is unburned because of extinguishment of the main flame, and a considerable fall in combustion efficiency takes place. Fig. 6 shows that the main flame blow-off limit which strongly depends on ϕ_{AF} in the inner flame, in contrast, depends on U_{mix} in the outer flame. This suggests that the blow-off mechanism on the inner flame is essentially different from that on the outer flame. In the case of transition from the normal flame to the crown flame, a low frequency oscillation is observed, the main flame existence alternates with the blow-off. Fig. 7 shows flame geometries of normal flame, crown flame and oscillatory flame.

The blow-off of the main flame is also observed, using different burner nozzles of 8, 14, and 20 mm inner diameter and varying U_2 and rim thickness^{1),8)}. Therefore, it can be concluded that the main flame blow-off as shown in Fig. 6 occurs over a wide range of flows and burner dimensions, in the premixed concentric jet flame with recirculation zone.

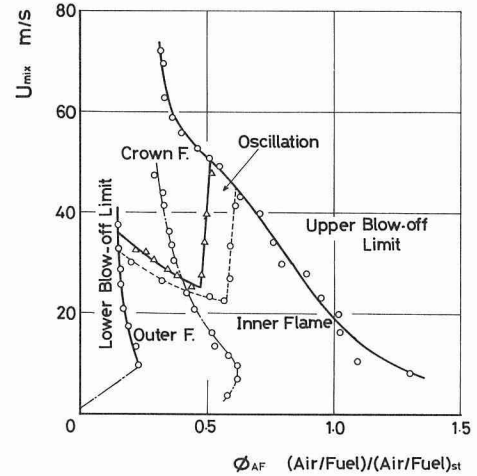


Fig. 6 Main flame stability limits ($U_2 = 35\text{m/s}$)

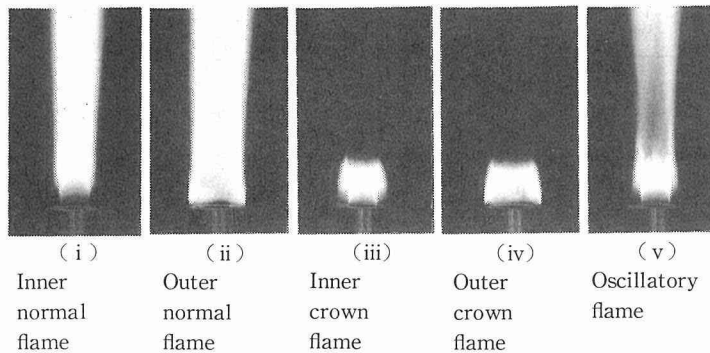


Fig. 7 Flame geometories

3. 2 Relations between thermal structure of recirculation zone and main flame stability

The recirculation zone has an essential role for the main flame stability. The zone is the source of heat and active species of the two outer flows, namely, the fresh mixture flow and the parallel air flow. The amount of heat and active species fed to the outer flows depends on the temperature in the zone. Then, detailed mean temperature distributions near the zone should be measured at both crown flame and normal

flame.

Fig. 8 shows the temperature distributions, for various ϕ_{AF} when $U_2 = U_{mix} = 35$ m/s. According to the classification of flame, these are referred to as inner flames. In this figure, y represents an axial distance from the burner exit, r represents a radial distance from the inner edge of the burner nozzle. The flame front is formed at FF as shown in the figure. Fig. 8 (a) shows a stable normal flame, (b) an oscillatory flame, (c) and (d) crown flames, respectively. In the normal flame (a) and the oscillatory flame (b), the maximum temperature region (over 1700 K) is narrow, and is located in the mixture side. On the other hand, the maximum temperature region covers almost all of the recirculation zone in the crown flame (c) and (d). The maximum temperature region stretches in the direction of downstream with an increase of ϕ_{AF} . The 1100 K region roughly covers the reaction zone of the recirculation zone. The resulting temperature profile, caused by the turbulent diffusion, can be seen as a 500 K region and is scarcely affected by ϕ_{AF} inside the flame.

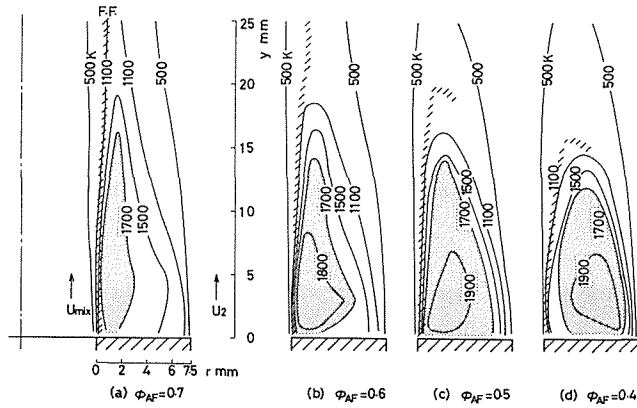


Fig. 8 Temperature distributions in recirculation zone ($U_2 = U_{mix} = 35$ m/s)

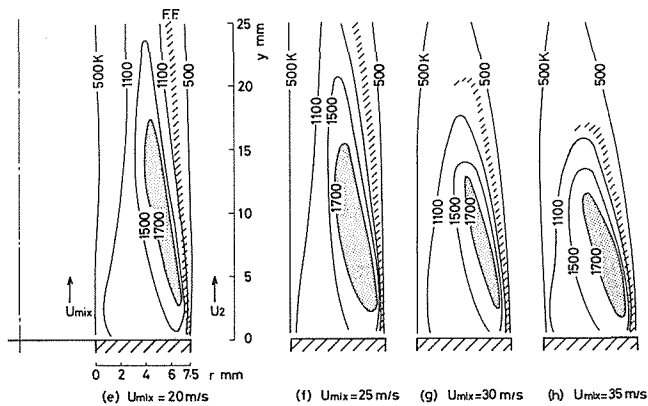


Fig. 9 Temperature distributions in recirculation zone ($U_2 = 35$ m/s, $\phi_{AF} = 0.3$)

Fig. 9 shows the temperature distributions for various U_{mix} , when $U_2=35$ m/s and $\phi_{AF}=0.3$. The Type of these flames is the outer flame. Fig. 9 (e) and (f) are normal flames, (g) and (h) are crown flames, respectively. The maximum temperature region stretches downstream with a decrease of U_{mix} . In addition, at the crown flame (g), the U_{mix} is slightly higher than the condition in which the main flame formed, and the 1100 K region is longer than in a typical crown flame (h). Generally, in the case of crown flames, the boundary of 500 K narrows with the increasing U_{mix} . This is attributed to the increase of U_{mix} that brings about an increase of the quantity of parallel air flowing into the recirculation zone.

From the temperature distributions described above, it is found that the maximum temperature and also the 1100 K region stretch downstream at the crown flame when the flame conditions approach the normal flame. It is assumed that the thermal structure of the recirculation zone at the crown flame, in which the maximum temperature region covers the zone, is most suitable for maintaining the main flame. However, the main flame actually blows off. This suggests that the main flame stability depends on the quantity of heat fed to the outer flows from the recirculation zone, and depends on ϕ_{AF} and the turbulent characteristics at the flame necking region.

3. 3 Reaction processes at flame necking region

Fig. 10 shows the radial profiles of mean temperature measured at flame necking region ($y=30$ mm) in the case of the stable normal flame ($U_2=35$ m/s, $U_{mix}=20$ m/s and $\phi_{AF}=0.3$), and in the near blow-off normal flame ($U_2=35$ m/s, $U_{mix}=25$ m/s and $\phi_{AF}=0.3$). The maximum temperature region is located inside the edge of outer flame front. The temperature decreases sharply away from the maximum temperature to the mixture side or the parallel air side. From a comparison of the two profiles, it is found that the maximum temperature decreases to about 200 K in the near blow-off flame.

Figs. 11 and 12 show the radial profiles of chemical species concentrations and local mixing ratio ϕ_{local} , under the same conditions as that in the mean temperature measurements. C_3H_8 is rapidly decomposed into CO and H_2 at the mixture side, after which, CO_2 is produced. The region where $\phi_{local}=1.0$ roughly corresponds to the maximum region of the temperature and CO_2 concentration.

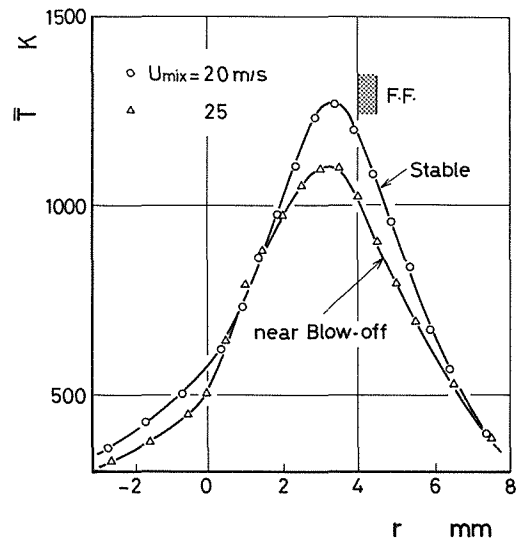


Fig. 10 Radial profiles of mean Temperature ($U_2=35$ m/s, $\phi_{AF}=0.3$, $y=30$ mm)

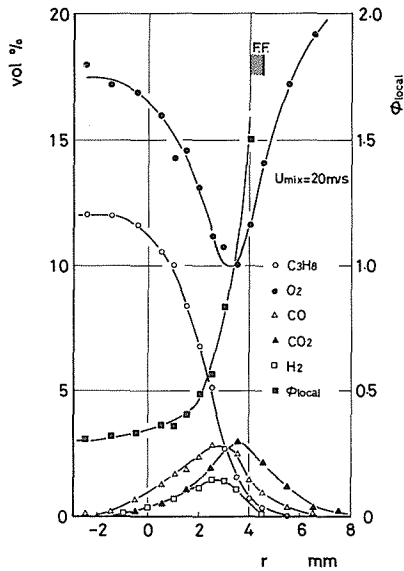


Fig. 11 Radial profiles of chemical species concentrations and local mixing ratio ϕ_{local} ($U_2=35\text{m/s}$, $\phi_{AF}=0.3$, $y=30\text{mm}$)

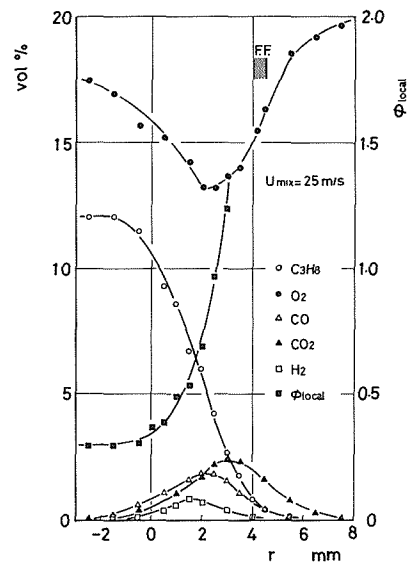


Fig. 12 Radial profiles of chemical species concentrations and local mixing ratio ϕ_{local} ($U_2=35\text{m/s}$, $\phi_{AF}=0.3$, $y=30\text{mm}$)

Comparing Fig. 11 and 12, it is found that CO and H₂ decrease and O₂ increases with the increasing U_{mix} . From the measurements of the mean temperature and species concentrations, it can be said that the burning fraction defined by the ratio of the supplied fuel and its consumption decreases at the near blow-off in the flame necking region.

The flame necking region corresponds to the place where the fresh mixture meets with the parallel air flow, so that in this shear region, a strong turbulence may exist. Therefore, the diffusion rate of the reactants is not negligible in comparison with the reaction rate, and quenching is easy to occur based on the finiteness of the reaction rate. An increase of turbulent intensity at the flame necking region with an increase of U_{mix} would be the most dominant factor of the decrease of the burning fraction.

3. 4 Microscopic structure at the flame necking region

Figs. 13 and 14 show the radial profiles of the time constant of the thermocouple used in this experiment. The measured time constants are scattered within several msec. This scattering in data is comparable to experimental accuracy, and the mean value of 13 msec. was selected as the circuit time constant throughout the experiment.

Fig. 15 shows the radial profiles of RMS value of temperature fluctuation measured at the stable and the near blow-off normal flame. RMS curve has two peaks of 60 K in the stable flame. One is located on the mixture side and the other on the parallel air side. The position of the peak on the air side corresponds to that of CO₂ peak

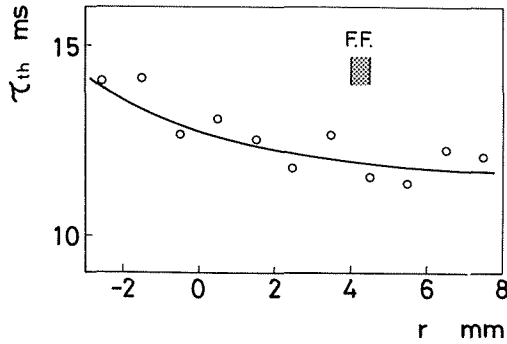


Fig. 13 Radial profile of thermocouple time constant
 ($U_2=35\text{m/s}$, $U_{mix}=20\text{m/s}$, $\phi_{AF}=0.3$,
 $y=30\text{mm}$)

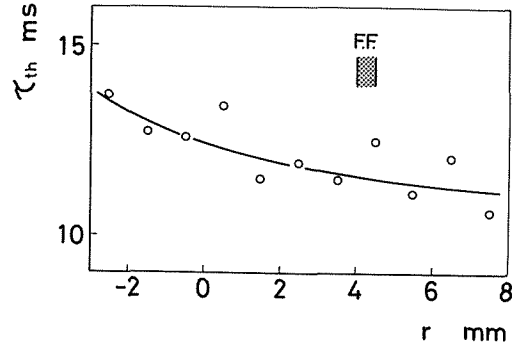


Fig. 14 Radial profile of thermocouple time constant
 ($U_2=35\text{m/s}$, $U_{mix}=25\text{m/s}$, $\phi_{AF}=0.3$,
 $y=30\text{mm}$)

and also to the outer edge of the flame front. On the parallel air side where the chemical reaction is nearly completed, temperature fluctuations are caused by the turbulent mixing of hot burnt gas and cold air as a result of a strong turbulence. On the other hand, on the mixture side, the temperature fluctuation is caused by the turbulent mixing of cold unburnt mixture and burnt gas, and by the onset of chemical reaction⁹.

In case of near blow-off flame, there is no RMS peak on the mixture side. The

decrease of mean temperature gradient and burning fraction may be considered for this reason. Fig. 16 shows a comparison of PDF measured at $y=2\text{mm}$. In the stable flame, the existence probability of the hot burnt gas

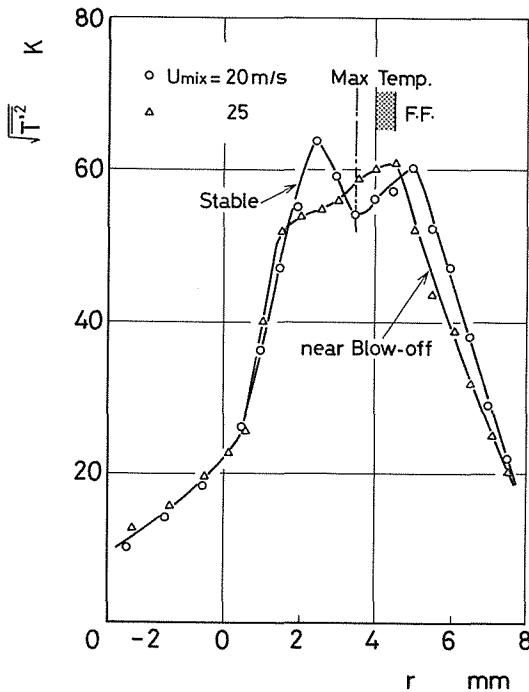


Fig. 15 Radial profiles of fluctuating temperature
 ($U_2=35\text{m/s}$, $\phi_{AF}=0.3$, $y=30\text{mm}$)

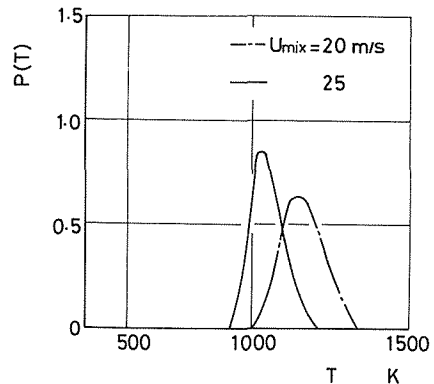


Fig. 16 Comparison of probability density functions
 ($U_2=35\text{m/s}$, $\phi_{AF}=0.3$, $y=30\text{mm}$, $r=2\text{mm}$)

is equal to that of cold mixture, because of PDF is of approximately the Gaussian type. In the case of near blow-off flame, the skewness of PDF is positive, so that cold unburnt gas is predominant. As described before, the phenomenon of the main flame blow-off is characterized by the decrease of RMS of the fluctuating temperature on the mixture side.

4. Conclusions

The main conclusions of the present study can be summarized as follows.

(1) The blow-off of the main flame is a phenomenon which occurs under a wide range of conditions of flows and burner dimensions in the premixed concentric jet flame with a recirculation zone. The blow-off in the case of the inner flame depends on ϕ_{AF} and in the outer flame depends on U_{mix} .

(2) In the case of normal flames, the maximum temperature region (over 1700 K) in the recirculation zone stretches downstream.

(3) The burning fraction at the flame necking region near blow-off condition decreases with the increasing U_{mix} .

(4) In the case of stable normal flames, RMS of the fluctuating temperature has two peaks, one on the mixture and one on the parallel air side. On the other hand, RMS decreases at the mixture side in the near blow-off normal flame.

Acknowledgement

The authors wish to express their thanks to Mr. T. Terada and Mr. Y. Arai for their assistance in this experiment.

References

- 1) Ito, K. Sasaki, M. and Fukasawa, S., JSME, 43-374, (1977), 3868.
- 2) Ito, K. and Sasaki, M., JSME, 44-383, (1978), 2478.
- 3) Saima, A., JSME, 26-168, (1960), 1144.
- 4) Mizutani, S. and Yano, K., JSME, 40-379, (1978), 1036.
- 5) Minx, E. and Kremmer, H., VDI-Berichte, 199, (1972), 78.
- 6) Ito, K. and Sasaki, M., JSME, 784-11, (1978), 120.
- 7) Shepard, C. E. and Warshawsky, I., NACA TN2703, (1952).
- 8) Ito, K. and Tanaka, H., Bulletin of Faculty of Engineering, Hokkaido Univ., 89, (1978), 29.
- 9) Lentz, W. and Günter, R., Comb. and Flame, 37, (1980), 63.